A FRAMEWORK FOR THE FUSION OF DIGITAL ELEVATION MODELS

H. Papasaika, D. Poli, E. Baltsavias

Institute of Geodesy and Photogrammetry, Swiss Federal Institute of Technology (ETH) Zurich, ETH-Hoenggerberg, CH-8093, Zurich, Switzerland, (haris,daniela.poli,manos) - @geod.baug.ethz.ch

Commission II, WG II/7

KEY WORDS: Multi-source data, Fusion, Integration, Quality Control, Spatio-temporal, Digital Elevation Model

ABSTRACT:

In recent years, collection and processing techniques for Digital Elevation Models (DEMs) generation have improved rapidly, allowing surfaces to be represented with more detail and accuracy. Fusion of overlapping DEMs, generated from data captured with different acquisition techniques, or from different times, allows to find inconsistencies, improve density, accuracy and currency, and eliminate gaps. This is of crucial importance for the improvement of global DEMs, like SRTM (Shuttle Radar Topography Mission). Since the DEMs may have substantial differences, simple amalgamation of all available points would not be satisfying and it would degrade the accuracy of the merged model. Any integration approach aiming at high-quality models needs an increased level of robustness. Computational efficiency and global convergence are further preferable properties. In this paper, an approach is presented for DEM fusion. The goal is to use existing DEMs to create automatically a new DEM surface which is: geometrically accurate by depicting the correct height information of the area, clean by eliminating blunders and errors which are present in the initial data and complete by modelling all the area on the highest possible resolution. The method is presented and the first results achieved after fusing a Lidar-based DEM and an IKONOS-based DEM on Thun, Switzerland, are shown and commented.

1. INTRODUCTION

The fusion of digital surfaces, that is their optimal combination into a new single dataset, is a crucial topic in the geomatic sciences. Nowadays, sensors and processing techniques provide for the same site Digital Elevation Models (DEMs) with different geometric characteristics and accuracy. Each DEM contains intrinsic errors due to the primary data acquisition technology and processing software methodology in relations with the particular terrain, and additional errors like blunders. In order to overcome the limitations of each surface model and create a better DEM, an intelligent fusion is required. Examples of situations where fusion is crucial are: merging of DEMs with similar accuracy generated by different techniques (for example, Lidar and image-based matching), update of a DEM with a more recent one, improvement of a global DEM (like SRTM) in areas where other DEMs are available for validation and elimination of erroneous points, removing systematic errors between DEMs.

However, although in technical literature some papers report DEMs fusion strategies, there is still not a consistent and global applicable solution on the topic of DEM fusion. The simplest approach, which is of combining all available points into one merged DEM, is not satisfactory (Hahn and Samadzadegan, 1999). In Gamba et al (2003) the fusion is applied combining InSAR DEMs or masking InSAR with LIDAR data, once 3D features are extracted. In Roth A. et al (2002) a technique to combine multi-source DEMs is outlined, which is based on the concept of height error maps. Podobnikar T. (2006) use a method based on the weighted sum of the data source for the integration of vector contour lines from maps, hydrographic elements and other characteristic lines, automatically derived characteristic lines and geodetic points. In James D.J. (2003) a tool in the ESRI software ArcInfo, with extension ArcGRID, is used with a seven-step methodology to fuse InSAR and Lidar DEMs.

The basic idea of our approach is to integrate different available height data according to their accuracy, which is described by a height error map. The goal of our fusion is to generate automatically a new DEM surface which is geometrically accurate by depicting the correct height information of the area, clean by eliminating blunders and errors which are present in the initial data and complete by modelling all the area in the highest possible resolution. Therefore, an accurate and reliable error map of each input surface model is required.

After the description of the fusion strategy, the accuracy of two DEMs located in Thun, Switzerland, and produced by image matching from IKONOS satellite images and airborne lidar scanning, is investigated and the first results of their fusion are reported and commented.

2. FUSION STRATEGY

To perform the fusion of multiple DEMs, the procedure shown in Figure 1 is proposed. The assumption is that we fuse two DEMs, called DEM1 and DEM2, with grid spacing s1 and s2, where s1>s2, and we produce a new DEM, called DEM3, with grid spacing s3. The only a priori information that we have for the DEMs DEM1 and DEM2 is their technology (i.e. laser, photogrammetry, SAR) and one global measure of accuracy. If the input surface models are available as point clouds, a regular grid is generated with grid size equal to the average point distance.
In order to fuse the DEMs and generate a new surface model with better accuracy, it is fundamental to have a complete knowledge of the characteristics and accuracy of the initial

DEMs. Each individual DEM is precisely evaluated by calculating a variety of quality measures.

Afterwards, the DEMs are aligned to a common reference system through co-registration (using often translations, rotations and a scale) and the 3D differences between the aligned surfaces are computed, as well as the corresponding X, Y, and Z components.

The following step is the generation of error maps, by exploiting the information from the residual maps and the accuracy analysis. Finally, the two DEMs are merged into DEM3 using a weighted average schema.

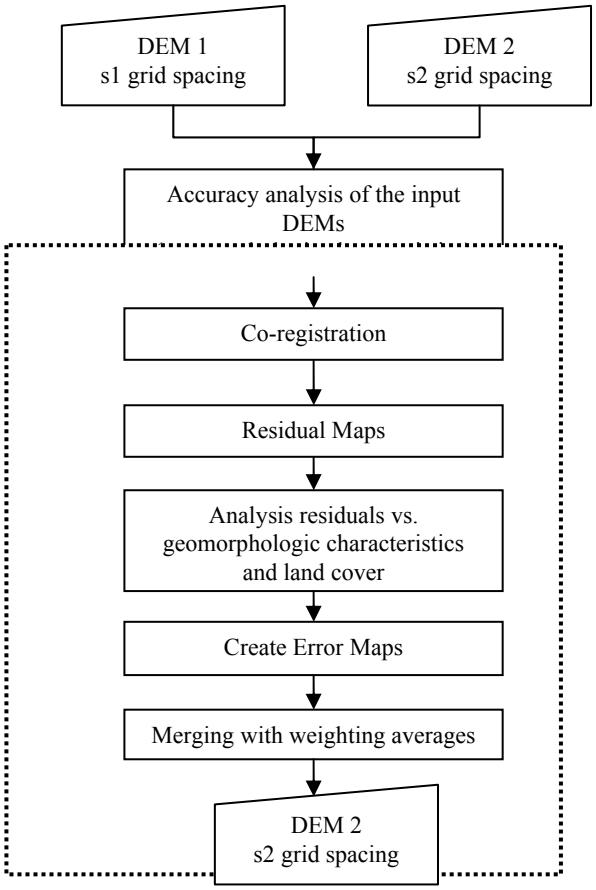

Figure 1. Workflow of the DEM fusion approach.

3. APPLICATION CASE STUDY

The study site is an area around the town of Thun, Switzerland, characterized by steep mountains, smooth hilly regions and flat areas. The elevation range is more than 1600m. The land cover is extremely variable with both dense and isolated buildings, open areas, forests, rivers and a lake. Over this test area, two IKONOS image triplets were acquired in October 2003, and a DEM was produced using image matching techniques with the ETH-IGP software Sat-PP at 4 m grid (Baltsavias et al., 2006). The estimated accuracy is 1-2m in open areas and about 3m on the average in the whole area, excluding vegetation. Another DEM was available from airborne lidar scanning. It is a 2m regular spacing DSM, with an accuracy of 0.5 m (1σ) for bare ground areas and 1.5m for vegetation and buildings. The lidar data were acquired in 2000 by the Swiss Federal Office of Topography, Bern (Swisstopo). In Table 1 the main characteristics of the two elevation models are given. The size of the overlapping area between the two DEMs is approximately 10km x 12km. Figure 2 shows the shaded DEM from IKONOS and details in the two test DEMs.

	Grid Spacing	Data Acquisition Date	Vertical Accuracy
Ikonos DEM	4 m	October 2003	1.0 m-5.0 m
Lidar DEM	2 m	2000	0.5 m-1.5 m

Table 1. DEMs main characteristics.

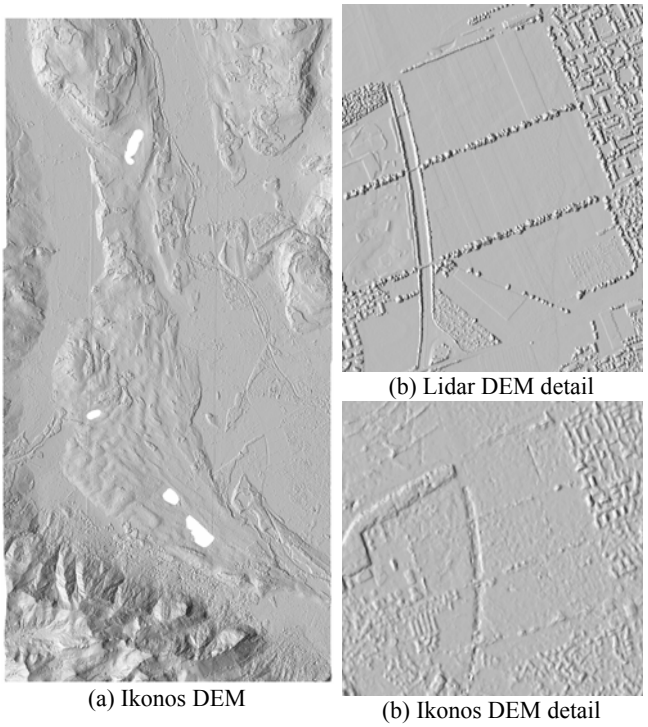

(a) Ikonos DEM

(b) Lidar DEM detail

(b) Ikonos DEM detail

Figure 2. (a) Ikonos DEM visualized in shaded mode with illumination angle 270°; (b) details in the lidar DEM and (c) in the Ikonos DEM.

4. ACCURACY ASSESSMENT

The quality of a DEM is difficult to be assessed rigorously. In addition, absolute measures of elevation error do not provide a complete assessment of DEM quality (Hutchinson and Gallant, 2000). If accurate reference DEM or surveyed ground data exist, standard statistical analysis can be performed. Otherwise, a number of alternative techniques for assessing data quality have been developed. These are non-classical measures of data quality that offer means of confirmatory data analysis without the use of an accurate reference DEM. Errors are also detected by comparing elevations with surrounding neighbours. Assessment of DEMs in terms of their representation of surface aspect has been examined by Wise (1998). Computing slopes and aspects allows a rapid inspection of the DEM for local anomalies. It can indicate both random and systematic errors. Other deficiencies in the quality of a DEM can be detected by examining frequency histograms of elevation and aspect.

4.1 Accuracy Parameters

Slope, aspect and roughness are the most important items for geomorphologic analysis of DEMs.
The common notion of the slope of a DEM *T(x,y)* is the amount of change in elevation in the steepest direction up or down the DEM. The slope function *S*(*x*, *y*) is defined as the magnitude of the first derivative of the DEM function *T*:

$$S(x,y) = \frac{360°}{2\pi}\arctan\left[\sqrt{\left(\frac{\partial T}{\partial x}\right)^2 + \left(\frac{\partial T}{\partial y}\right)^2}\right] \quad (1)$$

Aspect calculates the downhill direction of the steepest slope at each grid node. It is the direction that is perpendicular to the contour lines on the surface, and is exactly opposite the gradient direction. As with slope, aspect *A*(*x*, *y*) is calculated from estimates of the partial derivatives:

$$A(x,y) = 270° - \frac{360°}{2\pi}\arctan 2\left(\frac{\partial T}{\partial x}, \frac{\partial T}{\partial y}\right) \quad (2)$$

The algorithm used to determine slope and aspect uses a 3-by-3 neighbourhood around each cell in the elevation grid.
Roughness is a particular useful diagnostic tool because of its sensitivity to elevation alteration in the source DEM. There are many ways to calculate the roughness of the terrain (std. deviation, variance, fractal dimension). We experimented with all these methods and we found out that the entropy method performs better. The roughness of the DEMs is estimated locally by measuring the entropy. Entropy is a statistical measure of randomness that can be used to characterize the texture of the input DEM, *T*. Entropy *E*(*x*, *y*) is defined as

$$E(x,y) = -\text{sum}(\text{p}\cdot\log(\text{p})) \quad (3)$$

where p contains the histogram counts. Each output grid cell contains the entropy value of the n-by-n neighborhood around the corresponding grid cell in *T*. In our case, we use a neighborhood 9-by-9 (see Figure 3). For cells on the borders, symmetric padding is used.

4.2 Co-registration

The two DEMs are co-registered using a tool contained in the ETH-IGP semi-commercial software LS3D. The method performs 3D least squares matching between a 3D point cloud (slave) and a master point cloud, with any point density and accuracy (Gruen and Akca, 2005). The pair-wise LS3D matching is run on every overlapping dataset, setting as slave the DEM with the lower accuracy (in our case, Ikonos DEM) and as master the DEM (in our case, Lidar DEM) with the higher accuracy. Although LS3D generally uses a 7-parameter similarity transformation, in this case only 3 shifts were used, as the DEMs are referenced in the same geographic coordinate systems and there were no significant rotations or scale difference between them. The estimated shift parameters are 1.81m in X direction, -4.20m in Y direction and 0.76m in Z direction (sigma a priori was 5.0m, sigma a posteriori was 5.26m, 7 iterations). After the co-registration, the Euclidian distances (E) between the two DEMs are computed point-wise, together with the X, Y, Z components. The results are summarized in Table 2; positive differences indicate that the Ikonos DEM is above the lidar DEM. The largest errors are on the Z-component, but the shifts on the X and Y components are also significant. From the error distribution in Figure 3 we see that the larger discrepancies are mainly located on the south part, which is the steep mountain region.

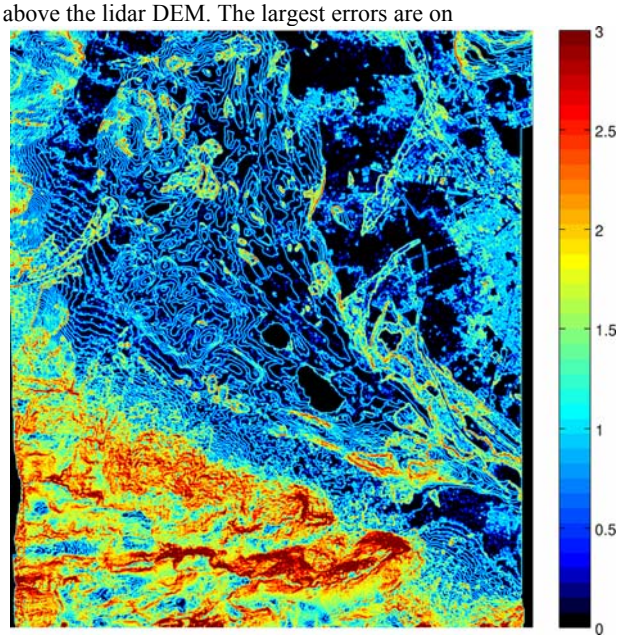

Figure 2. Roughness of the Ikonos DEM. Light to dark blue shows progressively regions with low roughness, i.e. valleys, water bodies. Light yellow to red show regions with high roughness, i.e. intense and abrupt elevation changes.

Some differences in the DEMs are due to the time difference between the acquisition time of the Ikonos images and the Lidar data, as shown in Figure 4. The light green to yellow color (positive differences) at the roads shows that the Ikonos DEM is higher, because matching at this image ground resolution mainly uses edge information from the surrounding building roofs to find corresponding points, while Lidar pulses are reflected at road level (see Figure 6). The blue color on the trees indicates that the trees are detected only on the lidar DEM.

			St. Dev. (m)	Mean (m)	Min (m)	Max (m)
lidar DSM	Ikonos DSM	E	5.92	-0.47	-127.57	116.3
		X	2.59	-0.11	-91.86	96.48
		Y	3.13	0.31	-61.51	95.88
		Z	4.30	-0.49	-99.26	69.80

Table 2. Statistical values of the Euclidean distances between Lidar DSM (template) and Ikonos DSM (search).

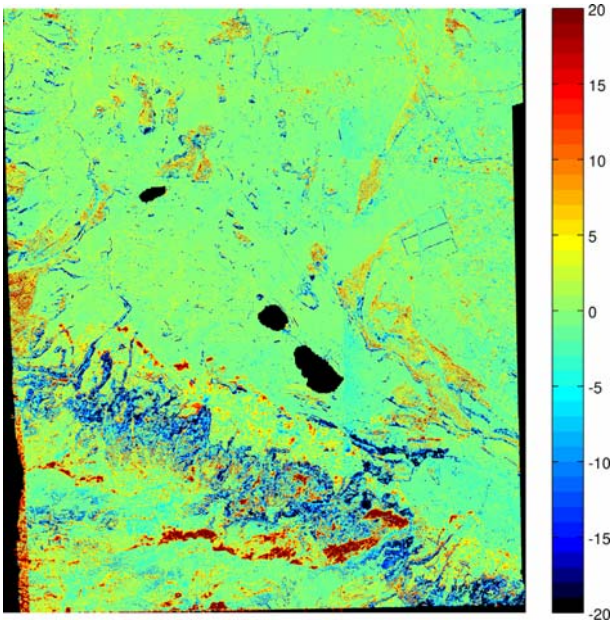

Figure 3. Euclidean (3D) residuals between the Ikonos and the Lidar DEMs. The biggest residuals are located on regions with steep slopes and in areas covered with forests.

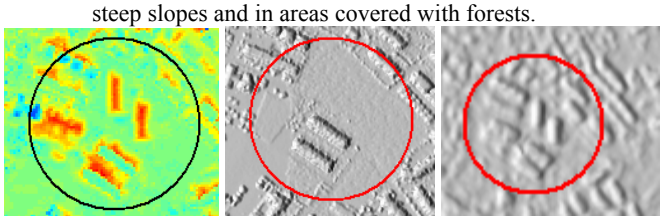

(a) 3D residuals (b) lidar DEM (c) Ikonos DEM

Figure 4. Example of temporal changes in the city of Thun. Some errors are due to new buildings in the Ikonos DEM (2003) that were not present in the Lidar DEM (2000).

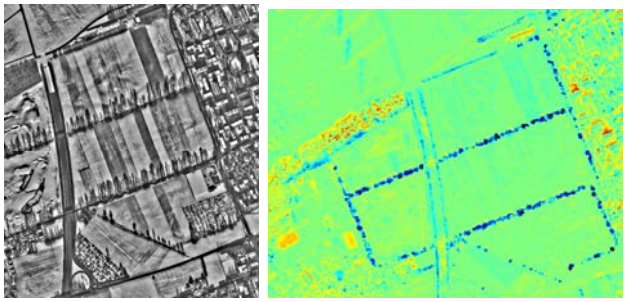

(a) Ikonos satellite image (b) Euclidean (3D) residuals

Figure 5. Snapshots from the Ikonos satellite image (a) and the Euclidean residuals map (b), where details are depicted from a big street and hedges.

4.3 Geomorphologic characteristics vs. residuals

The residuals between the DEMs were studied in relations to the geomorphologic characteristics of the terrain previously computed.

By plotting the residuals with respect to slope, aspect, and roughness (Figure 6), it can be noted that:

- The relief is one of the principal parameters to investigate the differences between the DEMs. In fact, the steeper the slope is, the larger the differences between the DEMs, whatever the aspect.
- Differences decrease consistently as roughness increases. In general, elevation accuracy and roughness are almost linearly correlated.
- NW and SE give generally the best and worse elevation differences, respectively. NW directions are facing mountain slopes in shadows and therefore they have large matching errors.
- Since these NE aspects face the IKONOS flight planning, these best results in the NE aspects in mountainous topography confirm the correlation between the flight path and the differences between the DEMs.

The above mentioned results demonstrate a combined correlation between elevation accuracy and terrain slope, aspect and roughness. It is therefore necessary to consider the geomorphologic characteristics in the fusion process.

5. FUSION

Having established the registration to a uniform coordinate system and identified the differences between the input surfaces, data integration can be carried out.

We combine height values from different DEMs using a weighted average rule. For the weights we generate the 3D error maps of each DEMs taking into account their theoretical (nominal) accuracy and the geomorphologic characteristics of the terrain. The fusion is applied in "problematic areas" where the differences between the two DEMs are significant with respect to their nominal accuracy. The grid size of the DEM3 is 2m, like that of Lidar DSM. The accuracy of the final surface will be predicted for each grid cell.

5.1 Error Map Generation

The height error is calculated for each grid point in the raster DEM and is stored in a matrix. Therefore, for each DEM the corresponding height error map has the same dimensions and grid size. The height error maps are generated according the residuals maps of the co-registration step and land cover maps, or aerial or satellite images. The weights are assigned according to three different error cases:

1. errors in localized patches of the input DEMs where systematic differences between the input surfaces exist.
2. contradictory height values at the same planimetric points of each surface.
3. random error, or noise.

In the first case, the weights are computed according to the nominal accuracy of the DEMs and the geomorphologic characteristics. In the second case, we chose as H3 the height of the DEM with the highest precision, or, in the case of a temporal series, most recent data. The third case is the most difficult and critical one. Random errors and noise should be detected, if possible, before the fusion. Otherwise these errors are propagated on the fusion product.

5.2 Weighted DEM Fusion

The mathematical formulation of the fusion is based on the weighted average. The height H_3 of DEM3 is calculated as:

$$H_3 = \frac{w_1 H_1 + w_2 H_2}{w_1 + w_2} \quad (4)$$

where H1 and H2 are the height values in DEM1 and DEM2 and w_1 and w_2 are the weights based on error maps E_1 and E_2 respectively. The advantage of this method is that the low weights prevent from the consideration of erroneous values.

The main disadvantage of this method is that already correct height values may be wrongly alternated. Furthermore, discontinuities are introduced on the resulting DEM. Further research should be done in order to examine the reliability of the weights and improve their calculation method.

6. APPLICATION

The fusion strategy has been tested on a small area. The weights are calculated as function of the geomorphologic characteristics slope and roughness. Three different approaches have been tested for the error map generation.

In the first experiment, the weights are inverse to the slope. If S_1 and S_2 are the slope grids of DEM1 and DEM2 respectively, then the corresponding weights are S_1^{-1} and S_2^{-1}. In the second experiment, the weights are proportional to the terrain roughness. If R_1 and R_2 are the roughness grids of DEM1 and DEM2 respectively, then the corresponding weights are R_1 and R_2. In the third experiment, the weights are a convolution of the slope and roughness, $S_1^{-1} * R_1$ and $S_2^{-1} * R_2$.

In Figure 6 the first results of the fusion are shown. On the lidar DEM higher values of slope are locally calculated in comparison to the Ikonos DEM because of the small grid spacing. In addition, the lidar DEM is much rougher because of the higher resolution more details are described, i.e. trees cannot be detected in the Ikonos DEM. In general, the slope and the roughness of the lidar DEM are more homogeneous and realistic because of the lidar technology. The image matching process used for the generation of the Ikonos DEM introduces in many regions noisy height values. Regarding the fusion results, the first test, using only slope dependent weights, produces roughly an "average" DEM. On the second test, using roughness dependents weights, many details are suppressed. The third fusion DEM, produced using as weights a combination of the roughness and the slope seems to be more complete, enhancing the lidar DEM with information taken from the Ikonos DEM.
The evaluation of the fusion results is only empirical at this moment. Additional test and comparisons should be done using reference data.

7. CONCLUSIONS AND FUTURE WORK

In this paper, we started from the accuracy assessment of different DEMs without a priori knowledge about their accuracy. We emphasized the problems due to the geomorphologic characteristics of the DEMs and we showed how it could be used to further enhance the data fusion procedure. Finally, we proposed some very simple algorithms to fuse lidar and photogrammetricaly produced DEMs over the same area, exploiting their characteristics. Although the weighted mean is a satisfactory averaging function more complex maximum likelihood estimators are available and should be tested. The use of land cover maps on the fusion area is necessary in order to understand the characteristics of the problematic areas and derive additional DEM quality measures. Specific problems like hole filling, discontinuities (aliasing) and blending will be addressed in the future.

ACKNOWLEDEGMENT

This work is part of PEGASE project (N° 30839), funded by the European Commission under the Sixth Framework Program. PEGASE (Pegase website, 2008) is a multidisciplinary European project involving 15 partners (industrial and academic) and it is headed by Dassault Aviation.

REFERENCES

Baltsavias E., Zhang L., Eisenbeiss H., 2006. DSM Generation and Interior Orientation Determination of IKONOS Images Using a Testfield in Switzerland. Photogrammetrie, Fernerkundung, *Geoinformation*, (1), pp. 41-54.

Buckley S.J., Mitchell H.L., 2004. Integration, validation and point spacing optimisation of digital elevation models. *The Photogrammetric Record*, 19 (108), pp. 277 – 295.

Esteban J., Starr A., Willetts R., Hannah P., Bryanston-Cross P., 2005. A Review of data fusion models and architectures: towards engineering guidelines. *Neural Computing and Applications*, 14(4), pp. 273-281.

Gallant J., Hutchinson M., Wilson J., 2000. Future directions for terrain analysis. Wilson, J., and Gallant, J. (eds), Terrain Analysis: Principles and Applications, New York :John Wiley and Sons: 423-426.

Gamba P., Dell'Acqua F., Houshmand B., 2003. Comparison and fusion of LIDAR and InSAR Digital Elevation Models over urban areas. *International Journal of Remote Sensing*, 24 (22), pp. 4289-4300, November.

Gruen A., Akca D., 2005. Least squares 3D surface and curve matching. ISPRS *Journal of Photogrammetry and Remote Sensing*, 59 (3), 151-174.

Hahn, M. and Samadzadegan, F., 1999. Integration of DTMs using wavelets. *International Archives of Photogrammetry and Remote Sensing*, 32(7-4-3W6): 90–96.

James D.J., 2003. Fusing LIDAR and IFSAR DEMs: a seven-step methodology, Topographic Engineering Center ERDC.

Pegase website, 2008. http://dassault.ddo.net/pegase.

Podobnikar T., 2006. DEM from various data sources and geomorphic details enhancement. Bohinj 2006 - 5th ICA Mountain Cartography Workshop.

Roth A., Knöpfle W., Strunz G., Lehner M., Reinartz P., 2002. Towards a Global Elevation Product: Combination of Multi-Source Digital Elevation Models. Proc. of *Joint International*

Symposium on Geospatial Theory, Processing and Applications, Ottawa, Canada.

Schultz H., Riseman E., Stolle F., Woo D-M., 1999. Error Detection and DEM Fusion Using Self-Consistency. *Seventh IEEE International Conference on Computer Vision*, Kerkyra, Greece, Sept. 20-25, Vo. 2, pp. 1174-1181.

Schultz H., Hanson A. R., Riseman E. M., Stolle F. R., Woo D., Zhu Z., 2002. A Self-consistency Technique for Fusing 3D Information. Invited talk presented at the *IEEE Fifth International Conference on Information Fusion*, Annapolis Maryland, July 7-11.

Wise S.M, 1998. The effect of GIS interpolation errors on the use of digital elevation models in geomorphology. In: Lowe, S.N., Richards, K.S. and Chandler, J.H. (eds), *Landform Monitoring, Modelling and Analysis*, John Wiley and Sons, 300 pp.

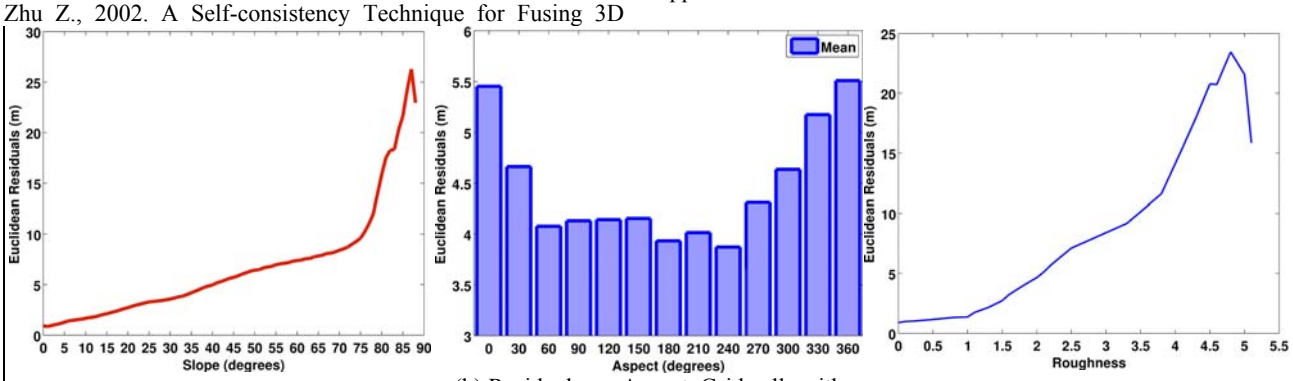

(a) Residuals vs. Slope.

(b) Residuals vs. Aspect. Grid cells with slope<10^o are rejected; 0º: North, 90º: East, 180º: South, 270º: West.

(c) Residuals vs. Roughness.

Figure 6. Plots of the 3D Euclidean residuals (mean values) as a function of the (a) slope, (b) aspect, and (c) roughness of Lidar DEM.

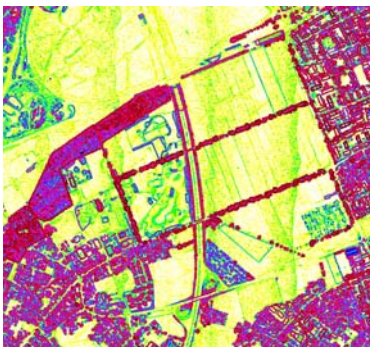

(a) Slope, lidar DEM

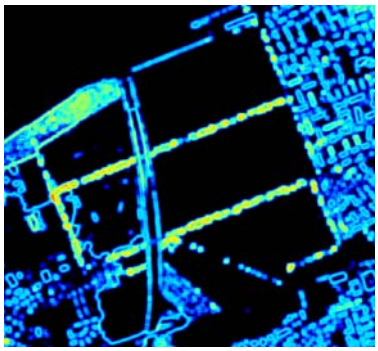

(b) Roughness, lidar DEM

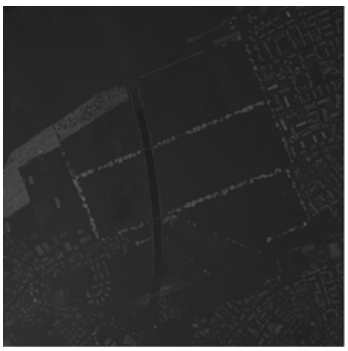

(c) lidar DEM

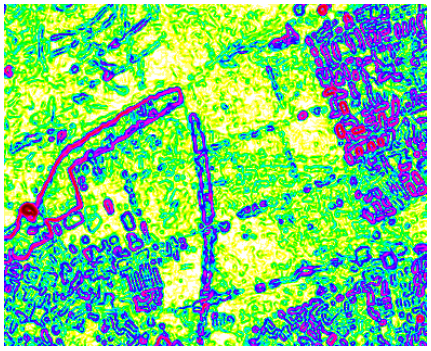

(d) Slope, Ikonos DEM

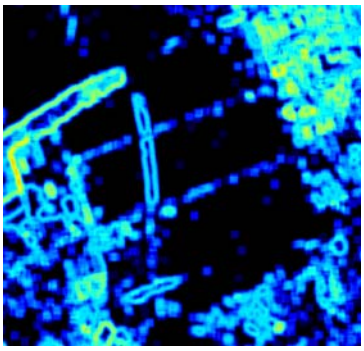

(e) Roughness, Ikonos DEM

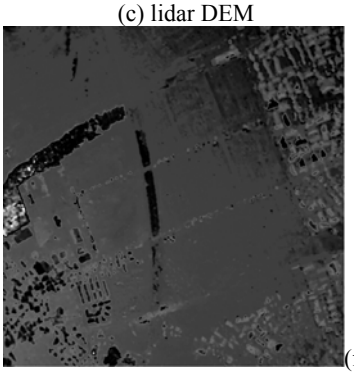

(f) Ikonos DEM

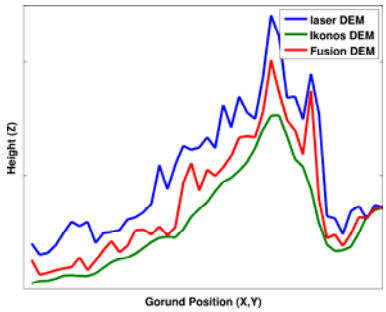

(g) Fusion, with slope dependent weights

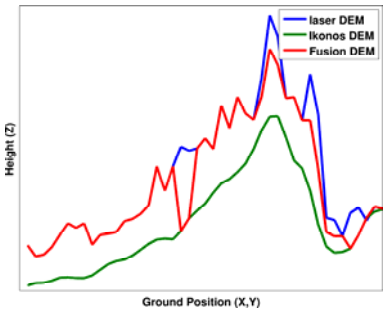

(h) Fusion, with roughness dependent weights

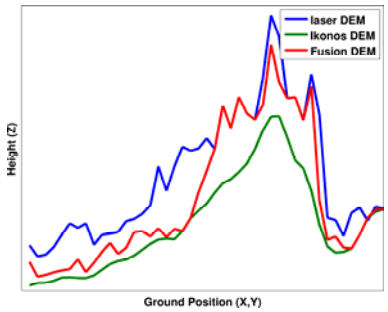

(j) Fusion, with slope and roughness dependent weights

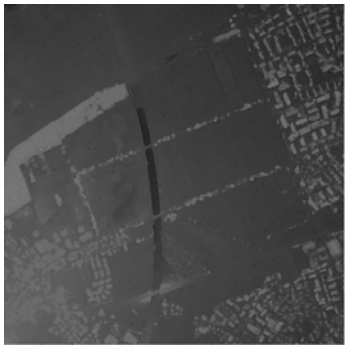

(i) Fusion, with slope dependent weights

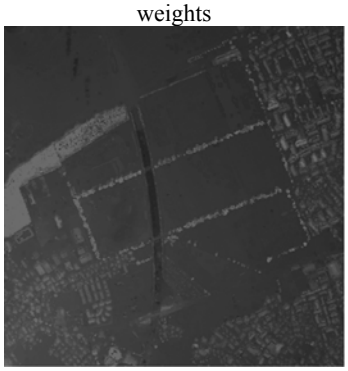

(k) Fusion, with roughness dependent weights

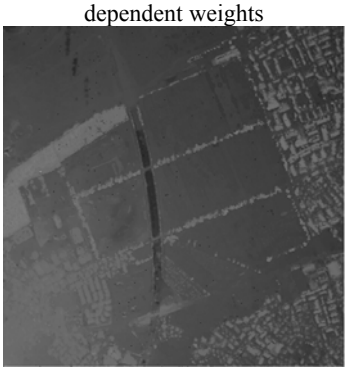

(l) Fusion, with slope and roughness dependent weights

Figure 7 First results of DEM fusion. The weights are dependent on the geomorphologic characteristics of slope and roughness. Slope values are progressively changing from white (plane areas) to red (steep slopes). Roughness values vary progressively from black (smooth areas) to blue (high textured areas). On the fourth line a 400 elevation points profile is selected to illustrate the result of the fusion. On the fifth line we see the results of the different fusion experiments.